ACS OMEGA

http://pubs.acs.org/journal/acsodf

Article

Physico-Chemical Structure and Gasification Performance of Co-Pyrolytic Char Produced by the Pyrolysis of Polyvinyl Chloride Blends with Two Rank Coals

Haiyu Meng,* Mengzhuo Wang, Zhiqiang Wu, Jun Zhao, Jiake Li, and Shuzhong Wang*

Cite This: *ACS Omega* 2022, 7, 32280−32291

Read Online

ACCESS | Metrics & More | Article Recommendations

ABSTRACT: Co-pyrolysis of waste plastics and coal has been considered to be an environmentally friendly and scalable waste treatment technology. This study investigated the influence of polyvinyl chloride (PVC) on the physico-chemical structure and gasification performance of co-pyrolytic char with lignite (PZ) and bituminous (SM) coal. The structure characteristics were explored by applying an X-ray diffractometer and a specific surface area analyzer. The quantitative analysis on the influence of PVC on pore characteristics and carbon microcrystal structure was conducted by the fractal theory and deconvolution method. The gasification performance was explored using a thermogravimetric analyzer. When the PZ blending ratio was larger than 50%, the specific surface area of PVCPZ chars enlarged significantly due to the increment of mesopores. Nevertheless, the effect of SM on the pore structure was not pronounced, and the specific surface area of PVCSM chars was as small as PVC char. A higher PZ blending ratio benefited the formation of mesopores with an aperture smaller than 10 nm for PVCPZ chars, whereas SM had little influence on pore diameter distributions of PVCSM chars attributed to the remarkable coating effects. The values of fractal dimension of co-pyrolytic char were larger than PVC char, revealing that the adjunction of coal increased the pore surface coarseness and improved the complicacy of the pore structure. Quantitative analysis on XRD spectra indicated that the disorder extent of the carbon structure was improved because of coal addition, and the influence of lignite on the disorder degree of the carbon structure was more significant. The gasification reaction of co-pyrolytic char showed significant synergistic effects, resulting in the improvement of gasification performance.

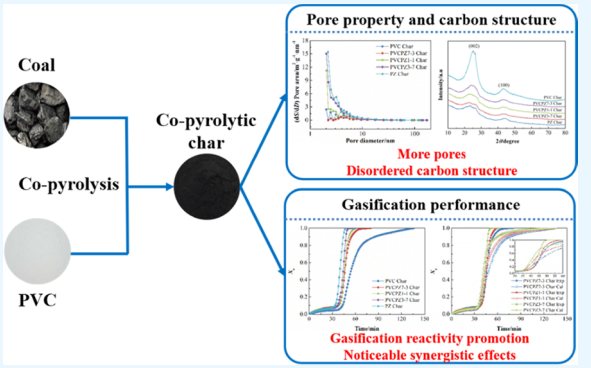

1. INTRODUCTION

The treatment of waste plastics has become a crucial issue because of the large consumption of plastic products in packaging, agriculture, industry, construction, and daily necessities.[1,2] Landfill is one of the common methods for waste plastics disposal currently. However, the landfill will occupy great amounts of valuable land, and the waste plastics degrade gradually because of their nondegradability.[3] The pollutants carried by waste plastics would contaminate groundwater as a result of rainwater washing.[4] The continuous landfill disposal of waste plastics will cause a large loss of recyclable resources and serious environmental issues.[5,6] Incineration, another conventional processing technique, can reduce the volume effectively and recover energy. In contrast, it is not considered a sustainable option attributed to the formation of harmful and toxic contaminants.[6,7] Consequently, developing efficient and clean treatment and utilization techniques for waste plastics is essential to environmental protection and resource recovery.

The production of fuel from waste plastics has gained extensive attention throughout the world. Fuel conversion from waste plastics can reduce the emissions of harmful substances compared with incineration and landfill treatment.[3] Pyrolysis/gasification, hydrothermal liquefaction, catalytic conversion, and advanced oxidation are the main methods for fuel production from waste plastics.[4,7] Among the existing techniques, pyrolysis seems to be the dominant way used, with the advantages of generating various products.[8,9] However, pure waste plastics cannot be converted into commercial-grade products on a plant scale by pyrolysis because of the low technical efficiency.[10,11] Co-pyrolysis with other solid fuels

Received: June 9, 2022
Accepted: August 22, 2022
Published: September 1, 2022

could be a solution for the high-efficient transformation of waste plastics.

Coal is the most widely used fossil fuel in China, and the common utilization method (combustion) of coal emits a massive amount of greenhouse gases.[12] Co-pyrolysis of waste plastics and coal has been regarded as a promising means to solve the problems in the pyrolysis process of waste plastics and reduce carbon emissions.[7,13] This approach has some advantages: the large-scale utilization of waste plastics, the partial substitution of fossil fuels in well-established industrial plant, the transformation of waste plastics to value-added products, as well as the quality improvement of pyrolysis products.[14−16] Additionally, the co-pyrolytic process is the inception phase of other co-thermochemical conversion techniques; thus, the characteristics of co-pyrolysis products have significant impacts on further reactions and their application.[17,18] In particular, the gasification or oxidation of co-pyrolytic solid products (char) is usually the rate-determining step of the thermochemical conversion process attributed to the lower reaction rate.[19−21] It is widely known that the physico-chemical structure (pore property, surface morphology, elementary compositions, carbon microcrystal structure, surface functional groups, and so forth) is the pivotal factor impacting the gasification performance of the char.[22−24] Co-pyrolysis of different solid fuels (coal, biomass, plastic, and so forth) would change the physico-chemical structure of the char,[25−27] then affecting their gasification performance. Therefore, it becomes significant to explore the impact of waste plastics on the physico-chemical structure property and gasification performance of co-pyrolytic char.

Some researchers have explored the physico-chemical structure of co-pyrolytic char from waste plastics and coal, particularly the pore property and carbon microcrystal structure, which are two significant factors impacting the gasification performance. In the char gasification process, the pores provide channels for the diffusion of gasification agents and reaction products, and the surface of pores is the primary adsorption site for the chemical reactions.[28,29] Thus, the characteristics of the pore structure have high influence on the gasification performance of co-pyrolytic chars. Sahu and Vairakannu executed an experimental research on co-pyrolysis of high-density polyethylene (HDPE) and bituminous coal.[8] The presence of HDPE increased the surface area of co-pyrolytic char obviously at 1000 °C but had a small influence on the surface area when the temperature was below 800 °C. Havelcova et al. reported that as the mass ratio of waste plastic (polyethylene terephthalate, PET) increased, the number of mesopores in char enlarged, but the number of micropores reduced.[30] The gasification performance of co-pyrolytic chars is also impacted by the ordered degree of the carbon microcrystal structure. Some investigators have reported the impact of waste plastics on the carbon microcrystal structure of co-pyrolytic char. Zhang et al. observed that the HDPE plastic could effectively accelerate the ordered degree of co-pyrolytic char with low-rank coal.[12] Havelcova et al. found that the PET plastic could promote the ordered degree of co-pyrolytic char at a relatively low plastic blending ratio. At the same time, the promoting effect was restrained at 20% plastic blending ratio.[30] Melendi et al. observed that the co-pyrolytic char produced by low-density polyethylene (LDPE) and coal blends was less aromatic with more C−H aliphatic bands.[31] The differences in the volatile matter content and chemical structure between waste plastics and coal would influence the pore and carbon structure of co-pyrolytic char, thus leading to the change in gasification performance.

The effects of different types of waste plastics (LDPE, HDPE, PET) on the physico-chemical structure of co-pyrolytic char have been investigated, and some valuable conclusions were obtained. It can be concluded that the type of waste plastics used was a pivotal factor in controlling the impact on the physico-chemical structure of co-pyrolytic char. Nevertheless, no report has been found on the influence of polyvinyl chloride (PVC) on the pore property and carbon structure of co-pyrolytic char with different rank coals. PVC plastic products are extensively used in various fields of industry and daily life, and the consumption of PVC occupies approximately 12% among the major kinds of plastics.[6,32] Large quantity of waste PVC is generated annually, and the efficient and clean processing has become a crucial concern. Thus, it is certainly worth exploring the physico-chemical structure and gasification performance of co-pyrolytic char from PVC/coal blends, which is very important to the design and optimization of the co-pyrolysis technique of waste plastics and coal.

The objective of this investigation is to reveal the effect of PVC on the physico-chemical structure and gasification performance of co-pyrolytic chars with two different rank coals. The pore structure properties of co-pyrolytic chars were quantitatively explored according to the fractal theory. The impact of PVC on the carbon structure of co-pyrolytic char was analyzed by fitting the diffraction peak of XRD patterns. Moreover, the gasification performance was explored, and the possible synergetic effects were also discussed. This research will provide some knowledge into deeper comprehension to co-pyrolysis of waste plastics and coal and supply scientific basis for the efficient and clean treatment and conversion of waste plastics.

2. MATERIALS AND METHODS

2.1. Materials. The PVC particles were bought from Aladdin Industrial Corporation. Two different rank coals in northern China were used to conduct the research, including lignite coal (PZ) and bituminous coal (SM). The basic characteristic analysis results of PVC and two kinds of coal are shown in Table 1. The characterization of PVC was performed by the ASTM standards for refused derived fuel (ASTM E790,

Table 1. Basic Characteristic Analysis Results of PVC and Two Kinds of Coal[a]

samples	PVC	SM	PZ
proximate analysis (wt %, ad)			
moisture	0	10.15	12.02
ash	0	5.95	24.25
volatile matter	92.14	31.06	38.32
fixed carbon	7.86	52.84	25.41
ultimate analysis (wt %, daf)			
carbon	39.66	78.89	69.81
hydrogen	5.24	3.09	4.72
nitrogen		1.07	1.24
sulfur	0.06	0.86	1.40
oxygen (by difference)		16.09	22.83
chlorine	55.04		
$Q_{net,ad}$ ($MJ \cdot kg^{-1}$)	20.38	26.57	18.79

[a]ad, air-dried basis; daf, dry and ash-free basis.

https://doi.org/10.1021/acsomega.2c03613
ACS Omega 2022, 7, 32280−32291

ASTM E830, and ASTM E897 for the proximate analysis; ASTM E777 for the analysis of carbon and hydrogen; ASTM E775 for the analysis of sulfur; ASTM E776 for the analysis of chlorine). The analysis of coals was carried out by the ASTM standards (ASTM D3172 for proximate analysis; ASTM D5373, ASTM D4239 for ultimate analysis). The air-dried materials with particle diameter smaller than 74 μm were selected to prepare pyrolytic char. The coal samples with a suitable size were obtained via grinding and sieving, and the PVC particles with an appropriate diameter were obtained through screening. The PVC/PZ mixtures were entitled as "PVCPZ3-7", "PVCPZ1-1", and "PVCPZ7-3", representing PVC/PZ mixtures with PVC mass ratios of 30, 50, and 70%, respectively. The PVC/SM mixtures were labeled as the same method. The mixtures were blended evenly by oscillating at 300 rpm for over 12 h.

2.2. Apparatus and Methods. *2.2.1. Char Preparation.* A fixed-bed tube reactor (internal diameter of 35 mm, length of 800 mm), warmed using an electric resistance oven, was employed to prepare the char samples in this investigation. First, high-purity nitrogen (99.999%) was introduced to purge the reactor, and the flow rate was 100 mL·min^{-1}. Then, the reactor temperature was elevated to 900 °C and remained unchanged for 10 min. Next, the raw materials were introduced into the reactor, and the pyrolysis experiments began. The pyrolysis gas was purged out of the reactor by the nitrogen, purified with a glass wool filter, a gas washer, and a silica gel drier one by one, and finally was collected. The duration of pyrolysis experiments was 15 min; then, the furnace was immediately turned off. When the reactor was reduced to ambient temperature, the char samples were finally gathered. The flow rate of purge gas remained unchanged throughout the experiment.

2.2.2. Pore Property Test and Fractal Analysis. The determination of pore properties of co-pyrolytic char was carried out using a specific surface area analyzer (Gold APP, V-Sorb 2800). The pore parameters were acquired according to the BET and BJH methods.[33−35] The complex pore structure of solid particles can be characterized using fractal dimension, a quantitative parameter based on the fractal theory.[36,37] It was found that the irregularity and complicacy of the pore structure of pyrolytic char from coal or biomass can be quantitatively explored by applying fractal theory because the char had the property of statistic self-similarity and scale invariance.[38] However, there is no investigation about fractal analysis on the pore structure of co-pyrolytic char from PVC blends with different rank coals. The fractal dimension (D) can be computed according to the following formula:[36]

$$\ln\left(\frac{V}{V_0}\right) = C + (D-3)\left[\ln\left(\ln\frac{P_0}{P}\right)\right] \tag{1}$$

where V represents adsorption quantity at a relative pressure (mL·g^{-1}), V_0 refers to saturated monolayer adsorption quantity (mL·g^{-1}), P_0 represents saturated vapor pressure of gas adsorption (Pa), P represents balanced pressure (Pa), and C refers to a constant. A high fractal dimension meant the char samples possessed an irregular porous structure and a rough pore surface.

2.2.3. Carbon Microcrystal Structure Analysis. X-ray diffraction (PANalytical, X'pert MPD) was employed to examine the carbon structure of co-pyrolytic chars. The carbon structure in char of carbon-based solid materials is composed of aromatic layers with multilayers stacking. The main parameters for characterizing carbon microcrystal structure include the crystal plane spacing (d_{002}), the crystallite size (L_a), and the average stacking height (L_c). The d_{002} reflects the distance between the aromatic layers. L_a refers to the length and width of the aromatic layer. L_c represents the average stacking thickness of each microcrystalline layer. The carbon microcrystal structure parameters can be computed based on Bragg and Scherrer equations normally.[39] The formulas are as follows:

$$d_{002} = \frac{\lambda}{2\sin\theta_{002}} \tag{2}$$

$$L_c = \frac{K_1\lambda}{\beta_{002}\cos\theta_{002}} \tag{3}$$

$$L_a = \frac{K_2\lambda}{\beta_{100}\cos\theta_{100}} \tag{4}$$

where d_{002} means crystal plane spacing (nm), L_c refers to average stacking height (nm), L_a represents crystallite size (nm), λ refers to the wavelength of X-ray (Å), θ refers to the angle of diffraction peak (°), β refers to the half-high width of diffraction peak (rad), and K represents the correction factor (CuKα, λ = 1.54178 Å, K_1 = 0.94, K_2 = 1.84).[40,41]

Previous research reported that three kinds of carbon structure usually existed in pyrolytic char: poor orientation structure, good orientation structure, and graphite-like structure.[41,42] These three kinds of carbon structures can be discriminated by fitting the diffraction peak (002) of XRD patterns. Wu et al. published that the carbon-containing substances of coal char can be separated into two types, microcrystalline structure with relatively poor orientation (P) and microcrystalline structure with relatively good orientation (G).[42] The quantitative parameters of these two forms of carbon structures can be obtained according to the following formulas:

$$d_{002,P} = \frac{\lambda}{2\sin(\theta_{002,P})} \tag{5}$$

$$d_{002,G} = \frac{\lambda}{2\sin(\theta_{002,G})} \tag{6}$$

$$L_{c,P} = \frac{K_1\lambda}{\beta_{002,P}\cos(\theta_{002,P})} \tag{7}$$

$$L_{c,G} = \frac{K_1\lambda}{\beta_{002,G}\cos(\theta_{002,G})} \tag{8}$$

where $d_{002,P}$ and $d_{002,G}$ refer to the crystal plane spacing of P and G peaks, respectively (nm), $L_{c,P}$ and $L_{c,G}$ refer to the average stacking height of P and G peaks, respectively (nm), λ represents the wavelength of X-ray (Å), $\theta_{002,P}$ and $\theta_{002,G}$ refer to the diffraction angle of P and G peaks, respectively (°), $\beta_{002,P}$ and $\beta_{002,G}$ refer to the half-high width of P and G peaks (rad), respectively. On this basis, the carbon structure parameters of co-pyrolytic chars were calculated using the weighted-average of corresponding parameters of these two carbon structures:

$$d_{002,m} = x_P d_{002,P} + x_G d_{002,G} \tag{9}$$

$$L_{c,m} = x_P L_{c,P} + x_G L_{c,G} \tag{10}$$

https://doi.org/10.1021/acsomega.2c03613
ACS Omega 2022, 7, 32280−32291

$$x_P = \frac{S_P}{S_P + S_G} \tag{11}$$

$$x_G = \frac{S_G}{S_P + S_G} \tag{12}$$

where $d_{002,m}$ represents average crystal plane spacing (nm), $L_{c,m}$ reflects the average stacking height (nm), x_P is the proportion of P peak area, x_G is the proportion of G peak area, S_P represents the area of P peak, and S_G represents the area of G peak. The value of L_a for co-pyrolytic char was obtained using eq 4, and the values of d_{002} and L_c were computed according to eqs 9 and 10.

2.2.4. Gasification Performance Test of Pyrolytic Char. The gasification performance of pyrolytic char was examined via a thermogravimetric analyzer (NETZSCH, STA2500). The mass of pyrolytic char used in each test was about 6 mg, and the gasification medium was high-purity carbon dioxide (99.999%) with a flow rate of 100 mL·min^{-1}. The test temperature was heated from 120 to 1050 °C and then held constant until the reaction finished. The heating rate used in the heating process was 20 °C·min^{-1}. The carbon conversion of pyrolytic char during gasification reaction was computed according to the following formula:

$$X_c = \frac{m_0 - m_t}{m_0 - m_a} \tag{13}$$

where X_c refers to experimental carbon conversion (%), m_0 represents the initial mass of pyrolytic char (mg), m_t represents the instantaneous mass of the char (mg), and m_a reflects the mass of pyrolytic char when the gasification test is completed (mg).

The gasification reactivity index (R_c) was calculated to characterize char reactivity. The formula is as follows:

$$R_c = \frac{1}{\tau_{0.5}} \tag{14}$$

where $\tau_{0.5}$ refers to the reaction time needed to reach X_c of 50% (min).

To explore if there exist synergetic effects on gasification reaction of co-pyrolytic chars from the blends of PVC and coal, the calculated carbon conversion ($X_{c,Calculated}$) of co-pyrolytic char was obtained according to eq 15:

$$X_{c,Calculated} = M_p X_{c,p} + M_c X_{c,c} \tag{15}$$

where M_p refers to PVC mass proportion in the blend (%), $X_{c,p}$ is the experimental carbon conversion of PVC char at the same gasification conditions (%), M_c refers to coal mass proportion in the blend (%), $X_{c,c}$ represents the experimental carbon conversion of coal char at the same gasification conditions (%). Positive synergetic effects accelerating the gasification reaction happened when the experimental results of carbon conversion of co-pyrolytic char demonstrated larger values than calculated results under the same gasification time. Otherwise, negative synergetic effects occurred when the calculated value was larger than the experimental value. Moreover, the synergistic effects were quantitatively evaluated by the root mean square (RMS) values of the differences between experimental and calculated carbon conversion. The RMS values can be obtained as follows:[43]

$$RMS = \sqrt{\frac{\sum_{i=1}^{n} (X_{c,Experimental} - X_{c,Calculated})^2}{n}} \tag{16}$$

where n represents the number of data points.

3. RESULTS AND DISCUSSION

3.1. Pore Properties of the Char. *3.1.1. Pyrolytic Char from PVC and Coals.* Figure 1 presents the N_2 isothermal adsorption curves of PVC char and coal chars. Although there existed a significant difference in adsorption capacity between the isothermal adsorption curves of PVC char and coal chars, they all showed an inverse S-shape. For pyrolytic char from PVC and coals, the isotherms both belonged to quintessential type II isotherms according to the classifying standard of IUPAC. Multimolecular layer adsorption on the surface of nonporous solids belonged to this type, which indicated that PVC char and coal chars from the pyrolysis process had a relatively continuous and complete pore distribution system. The pore diameter range was from molecular pores to infinite upper pores. A very complex pore structure was formed as a result of volatile matter releasing.

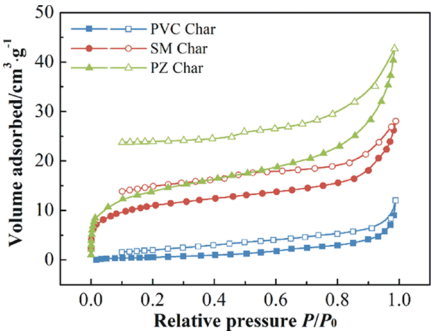

Figure 1. Isothermal adsorption curves of PVC char and coal chars.

It was shown in Figure 1 that within the range of relative pressure smaller than 0.1, the adsorption isotherms of these two coal chars first increased rapidly then increased slowly, showing an upward convex shape. It indicated that an apparent micropore filling phenomenon mainly occurred at lower relative pressure, and coal chars possessed profuse micropores and mesopores with a diameter of approximately 2 nm. When the relative pressure increased to above 0.1, the adsorption isotherms increased slowly with the enlargement of relative pressure. The N_2 adsorbed on the surface of pyrolytic chars gradually transited from the single-molecular layer to multimolecular layer. However, the adsorption isotherms increased sharply within the range of relative pressure higher than 0.8. It should be noted that there was no adsorption saturation phenomenon at relative pressure close to the saturated vapor pressure of adsorbate. The outcomes suggested that there existed certain amounts of mesopores and macropores in pyrolytic chars, and the phenomenon of macropore volume filling occurred due to the condensation of capillary pores. In the desorption process, the condensed liquid in capillary pores evaporated gradually with relative pressure reduction. However, because of the great difference in the specific shape of various capillary pores, there may be differences between the relative pressure of condensation and evaporation. Thus, the two branches of the isotherm would separate to form an adsorption loop. Different shapes of adsorption loops can

https://doi.org/10.1021/acsomega.2c03613
ACS Omega 2022, 7, 32280−32291

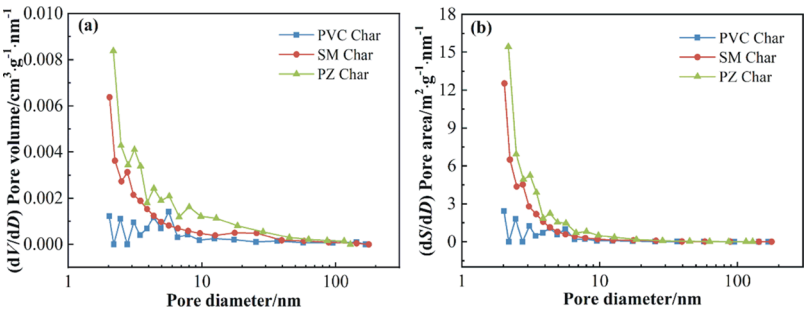

Figure 2. Pore diameter and specific surface area distributions of PVC char and coal chars.

Table 2. Pore Structure Parameters of PVCPZ Chars

chars	surface area/$m^2 \cdot g^{-1}$	pore volume/$cm^3 \cdot g^{-1}$	average pore size/nm	micropore volume/$cm^3 \cdot g^{-1}$	micropore surface area/$m^2 \cdot g^{-1}$	mesopore and macropore surface area/$m^2 \cdot g^{-1}$
PZ char	48.65	0.06609	9.38	0.00650	14.62	34.03
PVCPZ3-7 char	27.02	0.04251	8.29			27.02
PVCPZ1-1 char	10.39	0.02914	10.52			10.39
PVCPZ7-3 char	2.34	0.01404	15.45			2.34
PVC char	2.17	0.01862	15.10			2.17

Table 3. Pore Structure Parameters of PVCSM Chars

chars	surface area/$m^2 \cdot g^{-1}$	pore volume/$cm^3 \cdot g^{-1}$	average pore size/nm	micropore volume/$cm^3 \cdot g^{-1}$	micropore surface area/$m^2 \cdot g^{-1}$	mesopore and macropore surface area/$m^2 \cdot g^{-1}$
SM char	35.95	0.04342	9.30	0.00568	11.01	24.94
PVCSM3-7 char	4.82	0.01792	10.58			4.82
PVCSM1-1 char	3.15	0.01825	11.32			3.15
PVCSM7-3 char	3.07	0.01575	14.85			3.07
PVC char	2.17	0.01862	15.10			2.17

represent the pore structure of pyrolytic chars. The adsorption loops of these two coal chars were obvious, suggesting that coal chars had a more complex pore structure. The coal chars mainly contained impermeable and open holes, but not columniform holes. However, the adsorption isotherm of PVC char was obviously different from coal chars. The adsorption capacity of PVC char was almost unchanged with the relative pressure variation, and the isotherm did not form a significant adsorption loop. This finding implied that the pores in PVC char were primarily composed of capillary pores closed at one end and impermeable pores with wide variation in size.

Figure 2 illustrates the pore diameter and specific surface area distributions of PVC char and coal chars. Following the IUPAC classification standard,[44] the pores in solid porous particles can be divided into three categories by the size: macropores (d > 50 nm), mesopores (2 < d < 50 nm), and micropores (d < 2 nm). As displayed in Figure 2, the pore diameter and specific surface area distribution curves of PVC char and coal chars both presented an evident upward trend in the front part, which corresponded to the contribution of micropores and mesopores with a size less than 50 nm. However, when the pore size was greater than 50 nm, the distribution curves almost overlapped, revealing that the number of macropores in rapid pyrolytic chars was very small. The distribution curves of these two coal chars both showed a peak value at about 2 nm, revealing that the pores in coal chars were primarily composed of micropores and mesopores with size less than 10 nm. However, For PVC char, the curves of pore diameter and specific surface area distribution had no obvious peak value suggesting that the range of pore diameter was wide and uniform.

Tables 2 and 3 show the pore structure parameters of pyrolytic char. The PVC char showed a quite small specific surface area of 2.17 $m^2 \cdot g^{-1}$, and there were no micropores but mainly mesopores in PVC char. The average aperture of PVC char was about 15.10 nm. Nevertheless, the coal chars showed a significantly larger surface area than PVC char, respectively, 48.65 $m^2 \cdot g^{-1}$ for PZ char and 35.95 $m^2 \cdot g^{-1}$ for SM char. The mean pore size of PZ char and SM char were about 9.38 and 9.30 nm, respectively. The PVC char presented quite different pore characteristics from coal chars, which was related to the properties of raw materials. It was reported that the volatile matter of PVC has almost completely precipitated at the temperature below 600 °C;[6,45] then, a certain number of pores was formed at this temperature. With continuously rising temperature, the PVC char particles became soft and melted, leading to the collapse and blocking of some pores. Thus, the PVC char at 900 °C had a very small specific surface area attributed to the disappearance of micropores. Previous researchers also observed that biomass char had a relatively small surface area because of the pore fusion and void collapse at high temperatures.[46,47]

https://doi.org/10.1021/acsomega.2c03613
ACS Omega 2022, 7, 32280−32291

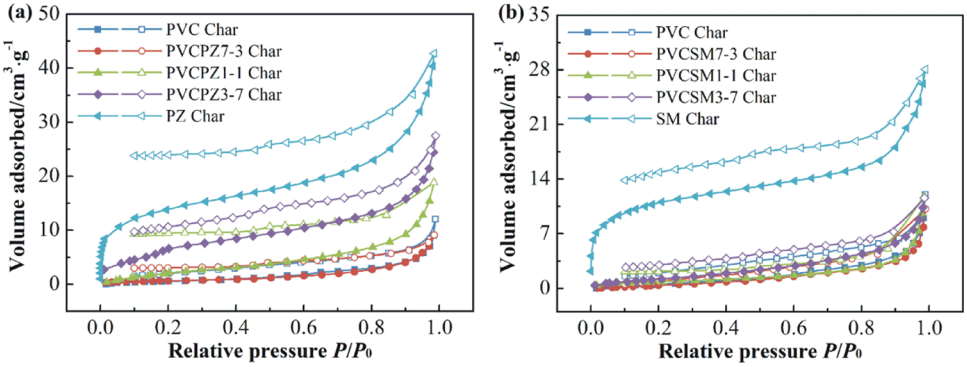

Figure 3. Isothermal adsorption curves of co-pyrolytic char: (a) PVCPZ chars and (b) PVCSM chars.

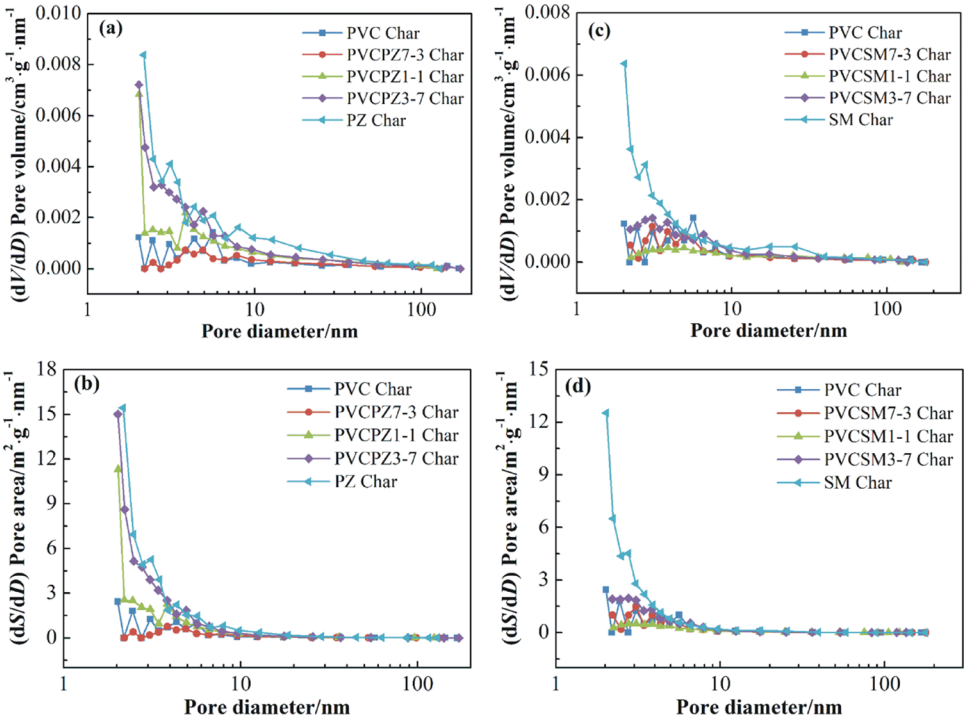

Figure 4. Pore diameter and specific surface area distributions of co-pyrolytic char: (a) and (b) PVCPZ chars (c) and (d) PVCSM chars.

3.1.2. Co-Pyrolytic Char from the Blends. The N_2 isothermal adsorption curves of co-pyrolytic char are presented in Figure 3. The isothermal adsorption curves of co-pyrolytic chars were also similar to type II isotherms. The change from monolayer adsorption to multilayer adsorption also occurred at the stage of relatively small relative pressure. With the further enlargement of relative pressure, the adsorption quantity increased slowly. However, the adsorption quantity of co-pyrolytic char samples enlarged quickly when the relative pressure was greater than 0.8. It was because the occurrence of the capillary pores condensation indicating that co-pyrolytic chars contained a certain amount of macropores and mesopores as same as the pyrolytic chars from individual samples. Like PVC char, the phenomenon of micropore filling did not happen in the initial stage of adsorption isotherms for co-pyrolysis chars, indicating that there were no micropores formed during the co-pyrolysis process. The morphology of adsorption isotherms of PVCPZ chars and PVCSM chars had little difference, but the adsorption capacity was quite different. The adsorption loop of PVCPZ7-3 char nearly overlapped with that of PVC char, and the adsorption capacity had little change. Nevertheless, the adsorption capacity of PVCPZ1-1 char and PVCPZ3-7 char magnified significantly with the continuous increment of the coal mixing ratio. In comparison with PVC char, the adsorption capacity of PVCSM chars at three blending ratios presented a small change, significantly different from PVCPZ chars. This meant that the PVCPZ chars had more abundant and developed pore structures than PVCSM chars. The pore properties of the char were the balanced results between newly increased pore volume in virtue of volatile matter releasing and the reduction of pore volume attributed to pore collapse and blockage.[48]

Figure 4 presents the pore diameter and specific surface area distributions of co-pyrolytic char. As illustrated in Figure 4a, b, the pore diameter distribution of PVCPZ chars presented significant change compared with PVC char and PZ char as well as the specific surface area distribution. These changes mainly took place in the range of mesopores with size less than 10 nm. When the PZ blending ratios were 50 and 70%, the number of pores with an aperture less than 10 nm in PVCPZ chars increased significantly compared with PVC char. Upon decreasing the PZ blending ratio to 30%, the pores with size

https://doi.org/10.1021/acsomega.2c03613
ACS Omega 2022, 7, 32280−32291

less than 10 nm decreased, and the pore diameter distribution tended to be uniform. However, the pore diameter and surface area distributions of co-pyrolytic char from blends with SM were analogous to PVC char, as presented in Figure 4c,d. The pore structures of PVCSM chars were not advanced, and the pore diameter distributions were broad and homogeneous. The change of the pore property can impact the reactivity of co-pyrolytic char because the pore structure mainly provides the adsorption site for chemical reactions and the mass transfer channel for gaseous phases.[28,29,49]

As displayed in Tables 2 and 3, the specific surface area of co-pyrolytic char declined as the PVC blending ratio enlarged. It was because the coating of molten plastic on the surface of coal particles would block holes and restrain the release of volatile matter.[16,50] Thus, the PVC addition would reduce the specific surface area of co-pyrolytic chars attributed to the destruction and collapse of some pores. It should be noted that there were no micropores in both co-pyrolytic chars from PVC blends with two different rank coals, but the specific surface area presented a different change trend. When the PVC blending ratio was 70%, the specific surface area of PVCPZ7-3 char was 2.34 $m^2 \cdot g^{-1}$, which was basically equal to PVC char. As the PVC blending ratio decreased to 50 and 30%, the surface area of PVCPZ chars enlarged obviously, and the values of the average pore diameter gradually decreased, which was due to the increase of mesopores with size less than 10 nm. Therefore, the conclusion was obtained that a higher PZ mixing ratio was beneficial to the pore formation for PVCPZ chars. However, the specific surface area of PVCSM chars at all three blending ratios was very small and close to PVC char. As we discussed earlier, the pore diameter distributions of PVCSM chars were broad and homogeneous. Thus, the PVCSM chars showed smaller pore volume and larger average pore diameter. It was probably because bituminous coal was more adhesive than lignite,[51,52] thereby the coating effects owing to plastic melting could bring a more remarkable impact on bituminous decomposition than lignite. For the co-pyrolytic process of PVCSM blends, the inhibitory effect on the release of volatile matter was stronger, and the pore plugging was more serious. As a result, the PVCSM chars had a very small specific surface area. The variation of pore structure parameters for co-pyrolytic chars was consistent with the change of pore diameter distributions.

3.1.3. Fractal Analysis on the Pore Structure of the Char. Table 4 presents the fractal dimension (D) of pyrolytic char. The R^2 indicated values larger than 0.94, demonstrating the reliability of calculation results. The value of D computed on the basis of N_2 adsorption data is between 2 and 3. The value of fractal dimension is 2, indicating a regular pore structure and smooth pore surface, while the value of 3 means an irregular porous structure and a rough pore surface.[29,53] It can be found that the D values of co-pyrolytic chars varied from 2 to 3 in this study, and the change trend of D values was consistent with the specific surface area. The coal chars presented larger D values than PVC char, revealing the pore structure of coal chars was more advanced and complex. The PVC would undergo a plastic deformation phenomenon during pyrolysis, which led to the pore destruction and slippery pore surface. As increasing coal mass ratio, the D values of co-pyrolytic chars enlarged. It can be concluded that the adjunction of coal increased the pore surface coarseness and improved the complicacy of the pore network structure.[29] Although PZ and SM coal both enhanced the pore structure development of co-pyrolytic chars, the effect of PZ on pore properties was more obvious than that of SM. Therefore, the D values of PVCSM chars were less than those of PVCPZ chars at the same blending ratio, indicating that PVCPZ chars had a more developed pore structure. Co-pyrolysis of PVC and coal can generate various chars with distinct pore properties by adjusting the coal type and blending ratios.

Table 4. Calculation Results of the Fractal Dimension of Pyrolytic Char

	PVCPZ char		PVCSM char	
PVC mass ratio	D	R^2	D	R^2
0	2.76	0.9990	2.72	0.9962
0.3	2.72	0.9820	2.53	0.9663
0.5	2.63	0.9813	2.44	0.9982
0.7	2.40	0.9796	2.40	0.9459
1	2.37	0.9444	2.37	0.9444

Figure 5 presents the relationship curve of the fractal dimension and the specific surface area for pyrolytic char. For PVCPZ chars and PVCSM chars, there was an exponential relationship between these two parameters. Wu et al. have also found an exponential relationship between these two parameters for co-pyrolytic chars produced by biomass and coal mixtures.[29] The fractal dimension considers the pore structure and surface characteristics, which can comprehensively characterize the pore properties in particles. The fractal study on the microscopic pore structure can supply quantitative knowledge about the stereoscopic degree of pores, which is helpful in deeply comprehending the impact of PVC on pore properties of the char produced by blends of waste plastics and coal.

3.2. Carbon Microcrystal Structure of the Char. Figure 6 illustrates the XRD patterns of pyrolytic char from individual and blended samples. For PVC char, coal chars, and co-pyrolytic chars, the basic morphology of the XRD pattern was similar, showing two broad peaks at diffraction angles between 20−30° (002 band) and between 40−50° (100 band). The 002 band was attributed to the graphite structure, and the existence of this band suggested the formation of the turbostratic carbon microcrystal structure in the char samples.[12] The (002) diffraction peak characterized the orientation degree of aromatic layers of the carbon microcrystal structure. The (100) band revealed the size of the aromatic layer of the carbon microcrystal structure. The variation of (002) and (100) peaks could indicate the ordered arrangement degree of the aromatic layer in microcrystalline structural units. The higher and narrower the (002) and (100) peaks are, the better the orientation degree of the aromatic layer and the larger the diameter of the aromatic layer (the higher the condensation degree of aromatic nucleus).[41,54] It can be found from Figure 6 that the (002) and (100) diffraction peaks of PVC char were more evident than those of coal chars, which indicated the generation of more ordered carbon structures like graphite in PVC char. The (002) diffraction peaks of co-pyrolytic chars became lower and wider as decreasing PVC mass ratio, which revealed the coal addition promoted the disorder extent of the carbon structure of co-pyrolytic char.

Table 5 presents the carbon crystalline structure parameters of pyrolytic char calculated based on the peak fitting analysis of the (002) diffraction peak. The $d_{002,m}$ value of PZ char was

https://doi.org/10.1021/acsomega.2c03613
ACS Omega 2022, 7, 32280−32291

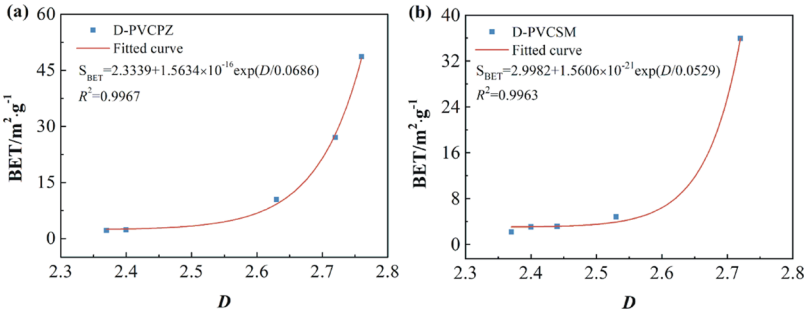

Figure 5. Relationship curve of the fractal dimension and surface area for co-pyrolytic char: (a) PVCPZ chars and (b) PVCSM chars.

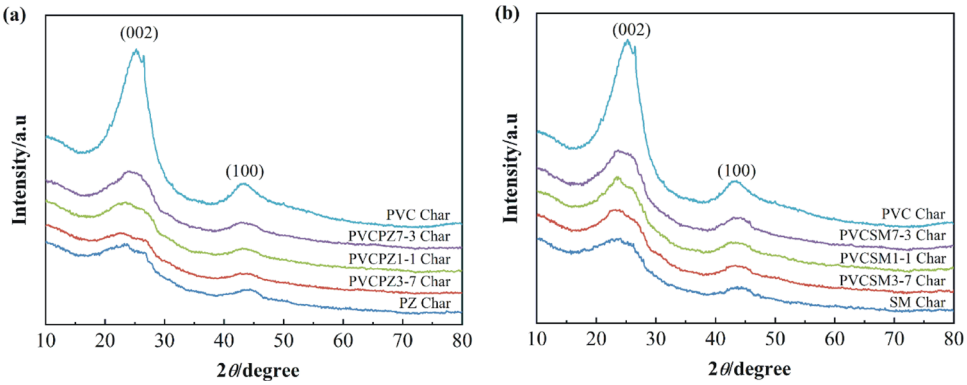

Figure 6. XRD patterns of co-pyrolytic char: (a) PVCPZ chars and (b) PVCSM chars.

Table 5. Carbon Crystalline Structure Parameters of Pyrolytic Char

chars	$d_{002,P}$/Å	$L_{c,P}$/Å	$d_{002,G}$/Å	$L_{c,G}$/Å	$d_{002,m}$/Å	$L_{c,m}$/Å	L_a/Å
PVC char	3.677	12.39	3.464	23.79	3.615	15.69	43.04
PVCPZ7-3 char	3.682	14.49	3.461	17.66	3.625	15.31	45.80
PVCPZ1-1 char	4.066	15.02	3.485	13.32	3.647	13.79	46.37
PVCPZ3-7 char	4.205	16.91	3.547	12.81	3.685	13.67	49.47
PZ char	4.399	15.09	3.625	13.94	3.741	14.12	41.46
PVCSM7-3 char	3.679	11.43	3.482	21.56	3.620	12.43	43.14
PVCSM1-1 char	3.668	10.99	3.622	14.65	3.639	11.76	44.07
PVCSM3-7 char	3.872	10.28	3.393	12.55	3.675	11.21	45.17
SM char	3.771	14.12	3.405	16.88	3.723	14.48	40.85

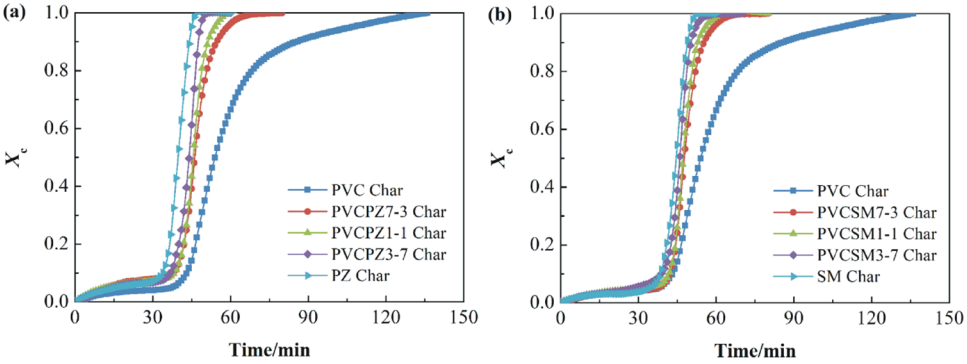

Figure 7. Carbon conversion during the gasification reaction of co-pyrolytic char: (a) PVCPZ chars and (b) PVCSM chars.

larger than SM char, which suggested that the carbon microcrystal structure of lignite char was less ordered compared with bituminous coal. This finding was consistent with the conclusion obtained by previous research.[55] For PVCPZ chars, the values of $d_{002,m}$ and L_a increased as the PVC mass ratio decreased, but the values of $L_{c,m}$ showed a converse variation tendency. The carbon microcrystal structure parameters of PVCSM chars presented a similar change trend to PVCPZ chars.

The variation tendency of carbon microcrystal structure parameters of the char revealed that the interlamellar spacing between the aromatic structures as well as the quantity of

https://doi.org/10.1021/acsomega.2c03613
ACS Omega 2022, 7, 32280−32291

interlayer defects between the adjacent aromatic units increased as the PVC mass ratio decreased.[29,41] Thus, the coal addition promoted the disorder degree of the carbon structure of co-pyrolytic char. With decrease in the PVC blending ratio, the free radical fragments produced by plastic cracking declined. Consequently, the quantity of free radicals absorbed on the char surface would reduce during pyrolysis, which was unfavorable to the condensation of aromatic rings.[56] This conclusion was consistent with the result obtained by previous research on the microcrystalline texture evolution of co-pyrolytic chars produced by HDPE and coal mixtures.[12] It can also be found that the $d_{002,m}$ values of PVCPZ chars were greater than those of PVCSM chars, indicating PVCPZ chars possessed a more disordered carbon microcrystal structure. It was reported that a good orientation degree of the carbon structure was unfavorable to the gasification reactivity of pyrolytic char because of the loss of marginal active sites.[57,58] Consequently, a highly disordered carbon microcrystal structure may improve the gasification performance of co-pyrolytic chars due to the increase of active sites.

3.3. Gasification Performance of the Char. The carbon conversion of co-pyrolytic char during gasification reaction is presented in Figure 7. The carbon conversion of PVC char was lower than coal chars at a fixed gasification time, indicating that PVC char was less reactive than coal chars. For co-pyrolytic chars, the carbon conversion was greater than PVC char at a constant gasification time, reflecting that the reactivity of co-pyrolytic chars was improved due to the coal addition. This was probably because co-pyrolytic chars had more pores and a more disordered carbon microcrystal structure than PVC char. As stated above, the surface area of PVCPZ chars enlarged due to the PZ adjunction, whereas the values of PVCSM chars were basically equal to PVC char. However, a more disordered carbon microcrystal structure was found for both PVCPZ and PVCSM chars compared with PVC char. The gasification performance of PVCPZ chars and PVCSM chars was both improved, indicating that the carbon microcrystal structure possessed a more remarkable impact on the gasification performance of co-pyrolytic chars. Moreover, the gasification performance promotion of co-pyrolytic chars was enhanced with increase in the coal blending ratio.

The gasification performance parameters of co-pyrolytic char are shown in Table 6. T_{gin} is the starting temperature of gasification reaction, and R_c represents the gasification reactivity index. The values of T_{gin} was obtained by the TG-DTG graphing method following the previous literature.[52,59] With the enlargement of the coal mass ratio, the T_{gin} values of co-pyrolytic chars decreased. According to the definition of R_c, the char with a higher R_c value meant higher gasification reactivity. The R_c of coal chars demonstrated larger values than PVC char, and the R_c values of co-pyrolytic chars increased with the improvement of the coal blending ratio. The larger R_c values indicated co-pyrolytic chars became more reactive compared with PVC char. It should be noted that the R_c values of PVCPZ chars were larger than those of PVCSM chars, revealing that the gasification performance of PVCPZ chars was better. It was because PVCPZ chars had more pores and a more disordered carbon microcrystal structure than PVCSM chars.

Table 6. Gasification Characteristic Parameters of Pyrolytic Char[a]

	PVCPZ char		PVCSM char	
PVC mass ratio	T_{gin}	R_c	T_{gin}	R_c
0	836	0.0252	884	0.0224
0.3	864	0.0227	907	0.0218
0.5	904	0.0219	929	0.0212
0.7	924	0.0216	949	0.0210
1	993	0.0185	993	0.0185

[a] T_{gin}, Starting temperature of gasification reaction/°C; R_c, Gasification reactivity index/min^{-1}.

The experimental and calculated carbon conversion of co-pyrolytic char is presented in Figure 8. The experimental carbon conversion of PVCPZ chars and PVCSM chars at a determined reaction time was less than the calculated values when the carbon conversion was small, revealing the occurrence of negative synergetic effects in the early stage of the gasification process. However, with growing carbon conversion, the experimental results presented larger values than the calculated results. The reaction time required for co-pyrolytic chars to reach the same carbon conversion decreased compared with the estimated time, demonstrating that positive synergetic effects took place during the later stage of the gasification reaction. Co-pyrolytic chars became more reactive, which is attributed to the occurrence of positive synergistic effects. Furthermore, the RMS values of the differences between experimental and calculated carbon conversion were 9.10, 8.22, and 6.83 for PVCPZ chars under the PVC mixing ratio of 30, 50, and 70%, respectively. Besides, the RMS values were 8.39, 6.65, and 4.52 for PVCSM chars under the PVC mixing ratio of 30, 50, and 70%, respectively. The higher the RMS values, the intense the synergistic effects.[43,60] From the results of RMS values, it can be concluded that noticeable synergistic effects occurred in the gasification reaction of co-pyrolysis chars, and the synergistic effects with lignite were more intense than bituminous coal at the same mixing ratio.

In the early stage of gasification reaction, the gasification process of co-pyrolytic was dominated by the gasification of coal char, showing that the experimental carbon conversion was lower than the calculated results. This was because the covering of molten plastic char restrained the diffusion of carbon dioxide and the release of volatiles in coal char particles. Consequently, the curves of experimental carbon conversion can be slightly delayed compared with the calculated curve. When the temperature increased to about 1000 °C, the gasification of coal char almost finished, and the gasification of PVC char began. The alkali and alkaline-earth metals (AAEMs) contained in coal char was kept in the samples. The AAEMs would produce catalysis impact on the following gasification reaction of PVC char at higher temperatures, leading to the positive synergistic effects in the later stage. Wang et al. investigated the oxidation reactivity of co-pyrolytic char from the blends of plastics and biomass and observed synergistic effects accelerating the reactivity attributed to the catalysis impact of potassium from biomass.[61] In addition, the gasification of coal char in the early stage would produce new pores in the plastic char enhancing the diffusion of gasification medium and reaction products, which was probably another cause for the promotion of the gasification performance of PVC char.

4. CONCLUSIONS

The physico-chemical structure and gasification performance of co-pyrolytic char produced by polyvinyl chloride (PVC)

https://doi.org/10.1021/acsomega.2c03613
ACS Omega 2022, 7, 32280−32291

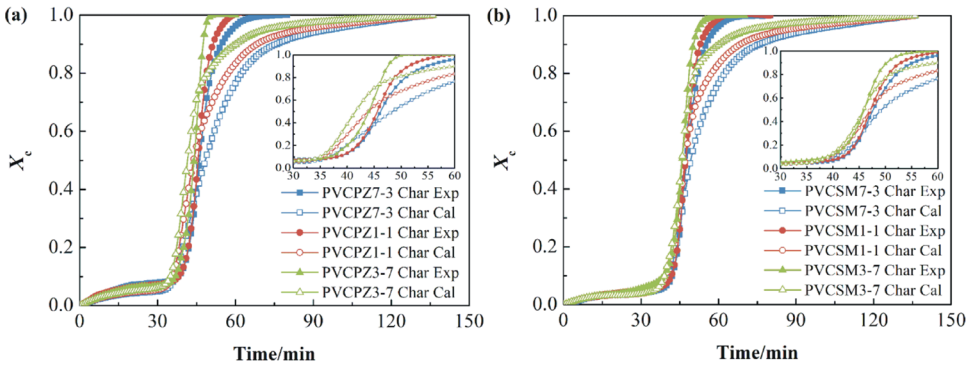

Figure 8. Experimental and calculated carbon conversion of co-pyrolytic char during gasification reaction: (a) PVCPZ chars, (b) PVCSM chars.

blends with bituminous (SM) and lignite (PZ) coal were explored in this work. The research results revealed that the pore characteristics of PVC char were obviously different from those of coal chars. There existed no micropores in PVC char, and the specific surface area was much smaller than coal chars. The pore diameter distribution of PVC char was broad and homogeneous. The addition of different rank coals had different impacts on the pore properties of co-pyrolytic chars. When the PZ blending ratio was greater than 50%, the specific surface area of PVCPZ chars enlarged significantly. Nevertheless, the specific surface area of PVCSM chars were basically equal to that of PVC char. A higher PZ blending ratio was favorable to the generation of mesopores with the pore size less than 10 nm for PVCPZ chars, but SM coal had little impact on pore diameter distributions of PVCSM chars because of the stronger coating effects. The fractal dimension of co-pyrolytic chars enlarged with increasing the coal mixing ratio, suggesting that the adjunction of coal increased the pore surface coarseness and improved the complicacy of the pore network structure. With increase in the coal mass ratio, the disorder degree of the carbon crystalline structure of co-pyrolytic char was increased. The effect of lignite on the disorder of co-pyrolytic chars was more significant than that of bituminous coal. The coal addition promoted the gasification reactivity of co-pyrolytic chars compared with PVC char. Synergistic effects were found on gasification reaction, and co-pyrolytic chars became more reactive due to the existence of synergistic effects. Lignite with higher blending ratios (more than 50%) was a better choice for high gasification reactivity char preparation for the co-pyrolysis process of PVC and coal.

AUTHOR INFORMATION

Corresponding Authors

Haiyu Meng − *Department of Municipal and Environmental Engineering, School of Water Resources and Hydro-Electric Engineering, Xi'an University of Technology, Xi'an, Shaanxi 710048, P.R. China;* orcid.org/0000-0003-0128-356X; Phone: +86-29-83239907; Email: hymeng321@163.com; Fax: +86-29-83239907

Shuzhong Wang − *Key Laboratory of Thermo-Fluid Science and Engineering, Ministry of Education, School of Energy and Power Engineering, Xi'an Jiaotong University, Xi'an, Shaanxi 710049, P.R. China;* orcid.org/0000-0002-0384-8993; Phone: +86-29-83239907; Email: szwang@aliyun.com; Fax: +86-29-83239907

Authors

Mengzhuo Wang − *Department of Municipal and Environmental Engineering, School of Water Resources and Hydro-Electric Engineering, Xi'an University of Technology, Xi'an, Shaanxi 710048, P.R. China*

Zhiqiang Wu − *Shaanxi Key Laboratory of Energy Chemical Process Intensification, School of Chemical Engineering and Technology, Xi'an Jiaotong University, Xi'an, Shaanxi 710049, P.R. China;* orcid.org/0000-0002-3067-014X

Jun Zhao − *Key Laboratory of Thermo-Fluid Science and Engineering, Ministry of Education, School of Energy and Power Engineering, Xi'an Jiaotong University, Xi'an, Shaanxi 710049, P.R. China*

Jiake Li − *Department of Municipal and Environmental Engineering, School of Water Resources and Hydro-Electric Engineering, Xi'an University of Technology, Xi'an, Shaanxi 710048, P.R. China*

Complete contact information is available at: https://pubs.acs.org/10.1021/acsomega.2c03613

Notes

The authors declare no competing financial interest.

ACKNOWLEDGMENTS

This work was financially supported by the Natural Science Basic Research Plan in Shaanxi Province of China (Grant No: 2018JQ5101), the China Postdoctoral Science Foundation (Grant No: 2018M633644XB), and the National Natural Science Foundation of China (Grant No: 51606149 and 51976168).

NOMENCLATURE

C	constant/−
D	fractal dimension/−
d_{002}	crystal plane spacing/nm
$d_{002,P}$	crystal plane spacing of P/nm
$d_{002,G}$	crystal plane spacing of G/nm
$d_{002,m}$	average crystal plane spacing of co-pyrolytic char/nm
K	correction factor/−
L_a	average crystallite size/nm
L_c	average stacking height/nm
$L_{c,P}$	average stacking height of P/nm
$L_{c,G}$	average stacking height of G/nm
$L_{c,m}$	average stacking height of co-pyrolytic char/nm
m_0	char mass at the beginning of experiment/mg
m_t	char instantaneous mass/mg

https://doi.org/10.1021/acsomega.2c03613
ACS Omega 2022, 7, 32280−32291

m_a	char mass when gasification test is completed/mg
M_p	PVC mass ratio in the blend/%
M_c	coal mass ratio in the blend/%
P	balanced pressure of gas/Pa
P_0	saturated vapor pressure of gas adsorption/Pa
R_c	gasification reactivity index/min^{-1}
S_P	the area of P peak/−
S_G	the area of G peak/−
T_{gin}	starting temperature of gasification reaction/°C
V	adsorption capacity at relative pressure/mL·g^{-1}
V_0	saturated monolayer adsorption quantity/mL·g^{-1}
x_P	proportion of P peak area/−
x_G	proportion of G peak area/−
X_c	carbon conversion/%
$X_{c,Calculated}$	calculated carbon conversion/%
$X_{c,p}$	carbon conversion of PVC char at same reaction condition/%
$X_{c,c}$	carbon conversion of coal char at same reaction condition/%
β	half-peak width of diffraction peak/rad
$\beta_{002,P}$	half-peak width of P peak/rad
$\beta_{002,G}$	half-peak width of G peak/rad
θ	angle of diffraction peak/°
$\theta_{002,P}$	angle of P peak/°
$\theta_{002,G}$	angle of G peak/°
λ	wavelength of X-ray/Å
$\tau_{0.5}$	time when the carbon conversion is 50%/min

Abbreviations

BET	Brunauer−Emmett−Teller
BJH	Barrett−Joyner−Halenda
HDPE	high-density polyethylene
IUPAC	International Union of Pure and Applied Chemistry
LDPE	low-density polyethylene
PET	polyethylene terephthalate
PVC	polyvinyl chloride
PVCPZ7-3	PVC/PZ blend with PVC mass ratio of 70%
PVCPZ1-1	PVC/PZ blend with PVC mass ratio of 50%
PVCPZ3-7	PVC/PZ blend with PVC mass ratio of 30%
PVCSM7-3	PVC/SM blend with PVC mass ratio of 70%
PVCSM1-1	PVC/SM blend with PVC mass ratio of 50%
PVCSM3-7	PVC/SM blend with PVC mass ratio of 30%
PZ	Pingzhuang lignite
SM	Shenmu bituminous
XRD	X-ray diffraction
P	microcrystalline structure with relatively poor orientation
G	microcrystalline structure with relatively good orientation

REFERENCES

(1) Lopez, G.; Artetxe, M.; Amutio, M.; Alvarez, J.; Bilbao, J.; Olazar, M. Recent advances in the gasification of waste plastics. A critical overview. *Renew. Sustain. Energy Rev.* **2018**, *82*, 576−596.

(2) Kumar, K. P.; Srinivas, S. Catalytic Co-pyrolysis of Biomass and Plastics (Polypropylene and Polystyrene) Using Spent FCC Catalyst. *Energy Fuels* **2020**, *34*, 460−473.

(3) Chen, R. Y.; Xu, X. K.; Zhang, Y.; Lo, S. M.; Lu, S. X. Kinetic study on pyrolysis of waste phenolic fibre-reinforced plastic. *Appl. Therm. Eng.* **2018**, *136*, 484−491.

(4) Li, N.; Liu, H. X.; Cheng, Z. N.; Yan, B. B.; Chen, G. Y.; Wang, S. B. Conversion of plastic waste into fuels: A critical review. *J. Hazard. Mater.* **2022**, *424*, No. 127460.

(5) Sharuddin, S. D. A.; Abnisa, F.; Daud, W.; Aroua, M. K. A review on pyrolysis of plastic wastes. *Energy Convers. Manag.* **2016**, *115*, 308−326.

(6) Yu, J.; Sun, L. S.; Ma, C.; Qiao, Y.; Yao, H. Thermal degradation of PVC: A review. *Waste Manag.* **2016**, *48*, 300−314.

(7) Kunwar, B.; Cheng, H. N.; Chandrashekaran, S. R.; Sharma, B. K. Plastics to fuel: a review. *Renew. Sustain. Energy Rev.* **2016**, *54*, 421−428.

(8) Sahu, P.; Vairakannu, P. CO2 based synergistic reaction effects with energy and exergy (2E) analysis of high density polyethylene with high ash bituminous coal for syngas production. *Fuel* **2022**, *311*, No. 122500.

(9) Cortazar, M.; Gao, N. B.; Quan, C.; Suarez, M. A.; Lopez, G.; Orozco, S.; Santamaria, L.; Amutio, M.; Olazar, M. Analysis of hydrogen production potential from waste plastics by pyrolysis and in line oxidative steam reforming. *Fuel Process. Technol.* **2022**, *225*, No. 107044.

(10) Samal, B.; Vanapalli, K. R.; Dubey, B. K.; Bhattacharya, J.; Chandra, S.; Medha, I. Char from the co-pyrolysis of Eucalyptus wood and low-density polyethylene for use as high-quality fuel: Influence of process parameters. *Sci. Total Environ.* **2021**, *794*, No. 148723.

(11) Du, S. H.; Yuan, S. Z.; Zhou, Q. Numerical investigation of co-gasification of coal and PET in a fluidized bed reactor. *Renewable Energy* **2021**, *172*, 424−439.

(12) Zhang, T. T.; Yuchi, W.; Bai, Z. Q.; Hou, R. R.; Feng, Z. H.; Guo, Z. X.; Kong, L. X.; Bai, J.; Meyer, B.; Li, W. Insight into the charging methods effects during clean recycling of plastic by co-pyrolysis with low-rank coal. *J. Clean. Prod.* **2022**, *333*, No. 130168.

(13) Hong, D. K.; Li, P.; Si, T.; Guo, X. ReaxFF simulations of the synergistic effect mechanisms during co-pyrolysis of coal and polyethylene/polystyrene. *Energy* **2021**, *218*, No. 119553.

(14) Melendi-Espina, S.; Alvarez, R.; Diez, M. A.; Casal, M. D. Coal and plastic waste co-pyrolysis by thermal analysis-mass spectrometry. *Fuel Process. Technol.* **2015**, *137*, 351−358.

(15) Saha, G. R.; Das, T.; Handique, P.; Kalita, D.; Saikia, B. K. Copyrolysis of Low-Grade Indian Coal and Waste Plastics: Future Prospects of Waste Plastic as a Source of Fuel. *Energy Fuels* **2018**, *32*, 2421−2431.

(16) Wu, Y. F.; Zhu, J. L.; Wang, Y. M.; Yang, H.; Jin, L. J.; Hu, H. Q. Insight into co-pyrolysis interactions of Pingshuo coal and high-density polyethylene via in-situ Py-TOF-MS and EPR. *Fuel* **2021**, *303*, No. 121199.

(17) Li, S. Q.; Song, H.; Hu, J. H.; Yang, H. P.; Zou, J.; Zhu, Y. J.; Tang, Z. Y.; Chen, H. P. CO_2 gasification of straw biomass and its correlation with the feedstock characteristics. *Fuel* **2021**, *297*, No. 120780.

(18) Zheng, X. Y.; Chen, W.; Ying, Z.; Jiang, Z. W.; Ye, Y. T.; Wang, B.; Feng, Y. H.; Dou, B. L. Structure-Reactivity Correlations in Pyrolysis and Gasification of Sewage Sludge Derived Hydrochar: Effect of Hydrothermal Carbonization. *Energy Fuels* **2020**, *34*, 1965−1976.

(19) Chen, X. Y.; Liu, L.; Zhang, L. Y.; Zhao, Y.; Qiu, P. H. Gasification reactivity of co-pyrolysis char from coal blended with corn stalks. *Bioresour. Technol.* **2019**, *279*, 243−251.

(20) Meng, H. Y.; Wang, S. Z.; Chen, L.; Wu, Z. Q.; Zhao, J. Study on product distributions and char morphology during rapid co-pyrolysis of platanus wood and lignite in a drop tube fixed-bed reactor. *Bioresour. Technol.* **2016**, *209*, 273−281.

(21) Strandberg, A.; Holmgren, P.; Wagner, D. R.; Molinder, R.; Wiinikka, H.; Umeki, K.; Brostrom, M. Effects of Pyrolysis Conditions and Ash Formation on Gasification Rates of Biomass Char. *Energy Fuels* **2017**, *31*, 6507−6514.

(22) Li, R. P.; Zhang, J. L.; Wang, G. W.; Ning, X. J.; Wang, H. Y.; Wang, P. Study on CO_2 gasification reactivity of biomass char derived from high-temperature rapid pyrolysis. *Appl. Therm. Eng.* **2017**, *121*, 1022−1031.

(23) Zhou, Y. J.; Zhu, S. H.; Yan, L. J.; Li, F.; Bai, Y. H. Interaction between CO_2 and H_2O on char structure evolution during coal char gasification. *Appl. Therm. Eng.* **2019**, *149*, 298−305.

https://doi.org/10.1021/acsomega.2c03613
ACS Omega 2022, 7, 32280−32291

(24) Wang, S.; Wu, L. P.; Hu, X.; Zhang, L.; Li, T. T.; Li, C. Z. Effects of the Particle Size and Gasification Atmosphere on the Changes in the Char Structure during the Gasification of Mallee Biomass. *Energy Fuels* **2018**, *32*, 7678−7684.
(25) Zhong, S. Y.; Zhang, B.; Liu, C. H.; Aldeen, A. S. Mechanism of synergistic effects and kinetics analysis in catalytic co-pyrolysis of water hyacinth and HDPE. *Energy Convers. Manag.* **2021**, *228*, No. 113717.
(26) He, Q.; Guo, Q. H.; Ding, L.; Gong, Y.; Wei, J. T.; Yu, G. S. Co-pyrolysis Behavior and Char Structure Evolution of Raw/Torrefied Rice Straw and Coal Blends. *Energy Fuels* **2018**, *32*, 12469−12476.
(27) Dong, Q.; Zhang, S. P.; Wu, B.; Pi, M.; Xiong, Y. Q.; Zhang, H. Y. Co-pyrolysis of sewage sludge and rice straw: thermal behavior and char characteristic evaluations. *Energy Fuels* **2020**, *34*, 607−615.
(28) Wang, G. W.; Zhang, J. L.; Chang, W. W.; Li, R. P.; Li, Y. J.; Wang, C. Structural features and gasification reactivity of biomass chars pyrolyzed in different atmospheres at high temperature. *Energy* **2018**, *147*, 25−35.
(29) Wu, Z. Q.; Ma, C.; Jiang, Z.; Luo, Z. Y. Structure evolution and gasification characteristic analysis on co-pyrolysis char from lignocellulosic biomass and two ranks of coal: Effect of wheat straw. *Fuel* **2019**, *239*, 180−190.
(30) Havelcova, M.; Bicakova, O.; Sykorova, I.; Weishauptova, Z.; Melegy, A. Characterization of products from pyrolysis of coal with the addition of polyethylene terephthalate. *Fuel Process. Technol.* **2016**, *154*, 123−131.
(31) Melendi, S.; Barriocanal, C.; Alvarez, R.; Diez, M. A. Influence of low-density polyethylene addition on coking pressure. *Fuel* **2014**, *119*, 274−284.
(32) Huang, Q. X.; Tang, Y. J.; Wang, S. R.; Chi, Y.; Yan, J. H. Effect of Cellulose and Polyvinyl Chloride Interactions on the Catalytic Cracking of Tar Contained in Syngas. *Energy Fuels* **2016**, *30*, 4888−4894.
(33) Brunauer, S.; Emmett, P. H.; Teller, E. Adsorption of gases in multimolecular layers. *J. Am. Chem. Soc.* **1938**, *60*, 309−319.
(34) Barrett, E. P.; Joyner, L. G.; Halenda, P. P. The determination of pore volume and area distributions in porous substances .1. computations from nitrogen isotherms. *J. Am. Chem. Soc.* **1951**, *73*, 373−380.
(35) Joyner, L. G.; Barrett, E. P.; Skold, R. The determination of pore volume and area distributions in porous substances .2. comparison between isotherm and mercury porosimeter methods. *J. Am. Chem. Soc.* **1951**, *73*, 3155−3158.
(36) Avnir, D.; Jaroniec, M. An isotherm equation for adsorption on fractal surfaces of heterogeneous porous materials. *Langmuir* **1989**, *5*, 1431−1433.
(37) Jaroniec, M. Evaluation of the fractal dimension from a single adsorption-isotherm. *Langmuir* **1995**, *11*, 2316−2317.
(38) Fu, P.; Yi, W. M.; Li, Z. H.; Bai, X. Y.; Wang, L. H. Evolution of char structural features during fast pyrolysis of corn straw with solid heat carriers in a novel V-shaped down tube reactor. *Energy Convers. Manag.* **2017**, *149*, 570−578.
(39) Yin, Y. S.; Zhang, J.; Sheng, C. D. Effect of pyrolysis temperature on the char micro-structure and reactivity of NO reduction. *Korean J. Chem. Eng.* **2009**, *26*, 895−901.
(40) Min, F. F.; Zhang, M. X.; Zhang, Y.; Cao, Y.; Pan, W. P. An experimental investigation into the gasification reactivity and structure of agricultural waste chars. *J. Anal. Appl. Pyrolysis* **2011**, *92*, 250−257.
(41) Wu, Z. Q.; Wang, S. Z.; Luo, Z. Y.; Chen, L.; Meng, H. Y.; Zhao, J. Physico-chemical properties and gasification reactivity of co-pyrolysis char from different rank of coal blended with lignocellulosic biomass: Effects of the cellulose. *Bioresour. Technol.* **2017**, *235*, 256−264.
(42) Wu, S. Y.; Gu, J.; Zhang, X.; Wu, Y. Q.; Gao, J. S. Variation of carbon crystalline structures and CO_2 gasification reactivity of Shenfu coal chars at elevated temperatures. *Energy Fuels* **2008**, *22*, 199−206.
(43) Wu, Z. Q.; Wang, S. Z.; Zhao, J.; Chen, L.; Meng, H. Y. Thermochemical behavior and char morphology analysis of blended bituminous coal and lignocellulosic biomass model compound co-pyrolysis: Effects of cellulose and carboxymethylcellulose sodium. *Fuel* **2016**, *171*, 65−73.
(44) Sing, K. S. W. Reporting physisorption data for gas solid systems - with special reference to the determination of surface-area and porosity. *Pure Appl. Chem.* **1982**, *54*, 2201−2218.
(45) Meng, H. Y.; Wang, S. Z.; Chen, L.; Wu, Z. Q.; Zhao, J. Investigation on synergistic effects and char morphology during co-pyrolysis of poly(vinyl chloride) blended with different rank coals from northern China. *Energy Fuels* **2015**, *29*, 6645−6655.
(46) Li, W. Y.; Wu, S. Y.; Wu, Y. Q.; Huang, S.; Gao, J. S. Gasification characteristics of biomass at a high-temperature steam atmosphere. *Fuel Process. Technol.* **2019**, *194*, 106090.
(47) Chang, C.; Liu, Z. H.; Li, P.; Wang, X. H.; Song, J. D.; Fang, S. Q.; Pang, S. S. Study on products characteristics from catalytic fast pyrolysis of biomass based on the effects of modified biochars. *Energy* **2021**, *229*, No. 120818.
(48) Meng, F. R.; Yu, J. L.; Tahmasebi, A.; Han, Y. N.; Zhao, H.; Lucas, J.; Wall, T. Characteristics of chars from low-temperature pyrolysis of lignite. *Energy Fuels* **2014**, *28*, 275−284.
(49) Zhang, X. S.; Bai, Y. H.; Wei, J. T.; Song, X. D.; Wang, J. F.; Yao, M.; Yu, G. S. Study on Char-Ash-Slag-Liquid Transition and Its Effect on Char Reactivity. *Energy Fuels* **2020**, *34*, 3941−3951.
(50) Zhou, L. M.; Luo, T. A.; Huang, Q. W. Co-pyrolysis characteristics and kinetics of coal and plastic blends. *Energy Convers. Manag.* **2009**, *50*, 705−710.
(51) Yan, W. P.; Chen, Y. Y. Interaction performance of co-pyrolysis of biomass mixture and coal of different rank. *Proc. CSEE* **2007**, *27*, 80−86.
(52) Meng, H. Y.; Wang, S. Z.; Chen, L.; Wu, Z. Q.; Zhao, J. Thermal behavior and the evolution of char structure during co-pyrolysis of platanus wood blends with different rank coals from northern China. *Fuel* **2015**, *158*, 602−611.
(53) Chen, J.; Fang, D. D.; Duan, F. Pore characteristics and fractal properties of biochar obtained from the pyrolysis of coarse wood in a fluidized-bed reactor. *Appl. Energy* **2018**, *218*, 54−65.
(54) Yu, J.; Sun, L. S.; Berrueco, C.; Fidalgo, B.; Paterson, N.; Millan, M. Influence of temperature and particle size on structural characteristics of chars from Beechwood pyrolysis. *J. Anal. Appl. Pyrolysis* **2018**, *130*, 127−134.
(55) Wang, B.; Sun, L. S.; Su, S.; Xiang, J.; Hu, S.; Fei, H. Char Structural Evolution during Pyrolysis and Its Influence on Combustion Reactivity in Air and Oxy-Fuel Conditions. *Energy Fuels* **2012**, *26*, 1565−1574.
(56) Zhang, S.; Min, Z. H.; Tay, H. L.; Asadullah, M.; Li, C. Z. Effects of volatile-char interactions on the evolution of char structure during the gasification of Victorian brown coal in steam. *Fuel* **2011**, *90*, 1529−1535.
(57) Tay, H. L.; Li, C. Z. Changes in char reactivity and structure during the gasification of a Victorian brown coal: comparison between gasification in O_2 and CO_2. *Fuel Process. Technol.* **2010**, *91*, 800−804.
(58) Li, Y.; Yang, H. P.; Hu, J. H.; Wang, X. H.; Chen, H. P. Effect of catalysts on the reactivity and structure evolution of char in petroleum coke steam gasification. *Fuel* **2014**, *117*, 1174−1180.
(59) Wang, C. A.; Du, Y. B.; Che, D. F. Reactivities of coals and synthetic model coal under oxy-fuel conditions. *Thermochim. Acta* **2013**, *553*, 8−15.
(60) Sadhukhan, A. K.; Gupta, P.; Goyal, T.; Saha, R. K. Modelling of pyrolysis of coal-biomass blends using thermogravimetric analysis. *Bioresour. Technol.* **2008**, *99*, 8022−8026.
(61) Wang, X. B.; Ma, D. Y.; Jin, Q. M.; Deng, S. H.; Stancin, H.; Tan, H. Z.; Mikulcic, H. Synergistic effects of biomass and polyurethane co-pyrolysis on the yield, reactivity, and heating value of biochar at high temperatures. *Fuel Process. Technol.* **2019**, *194*, 106127.

https://doi.org/10.1021/acsomega.2c03613
ACS Omega 2022, 7, 32280−32291